# scientific reports



# **OPEN** Unraveling anthelmintic targets and mechanisms of action of transcinnamaldehyde from cinnamon essential oil

Guillermina Hernando<sup>®</sup>, Ornella Turani<sup>®</sup>, Noelia Rodriguez Araujo<sup>®</sup>, Alcibeth Pulido Carrasquero & Cecilia Bouzat

Parasitic nematodes pose a significant global socio-economic threat and contribute to neglected diseases. Current infection control relies on drug therapy, but increasing anthelmintic resistance highlights the urgent need for novel treatments. In this study, we investigate the molecular targets and mechanisms of action of trans-cinnamaldehyde (TCA), a principal component of Cinnamon Essential Oil (Cinnamomum verum EO), using Caenorhabditis elegans as a model organism. Our research offers new insights into the anthelmintic effects of TCA by identifying its specific interactions with key Cys-loop receptors and detailing its inhibitory mechanisms. The anthelmintic activity of C. verum EO and TCA manifests as rapid alterations in locomotor activity and inhibition of egg hatching. TCA screening of mutant worms lacking Cys-loop receptors reveal multiple receptor targets, including the levamisole-sensitive nicotinic ACh receptor (L-AChR), GABA-activated chloride channel (UNC-49) and glutamate-activated chloride channel. The mechanism behind the egg hatching inhibition by TCA remains unclear, as none of the mutants studied were found to be resistant to TCA. Furthermore, TCA increases the paralyzing effects of the anthelmintics levamisole and monepantel in a synergistic manner, offering a route for more effective polytherapy strategies. Electrophysiological studies on C. elegans Cys-loop receptors, in both native and heterologous systems, were used to elucidate the molecular mechanisms of TCA-induced paralysis. TCA reduces ACh- and GABA-elicited macroscopic currents and decreases single-channel activity and open durations of native muscle L-AChR channels, indicating an inhibitory action. Thus, by acting through a different mechanism to that of classical anthelmintics, TCA may be beneficial to counteract resistance in combined anthelmintic therapies. Our findings underscore the potential of the multitarget compound TCA as a valuable tool in integrated pharmacological strategies.

**Keywords** Cinnamomum verum essential oil, Trans-cinnamaldehyde, Anthelmintic drug, Cys-loop receptor, Electrophysiology, Caenorhabditis elegans

#### Abbreviations

EO

UNC-49 Gamma-aminobutyric acid (GABA)-activated chloride channel

GluCl Glutamate-activated chloride channels

IVM Ivermectin

L-AChR Levamisole-sensitive nicotinic acetylcholine receptor

LEV Levamisole MNP Monepantel

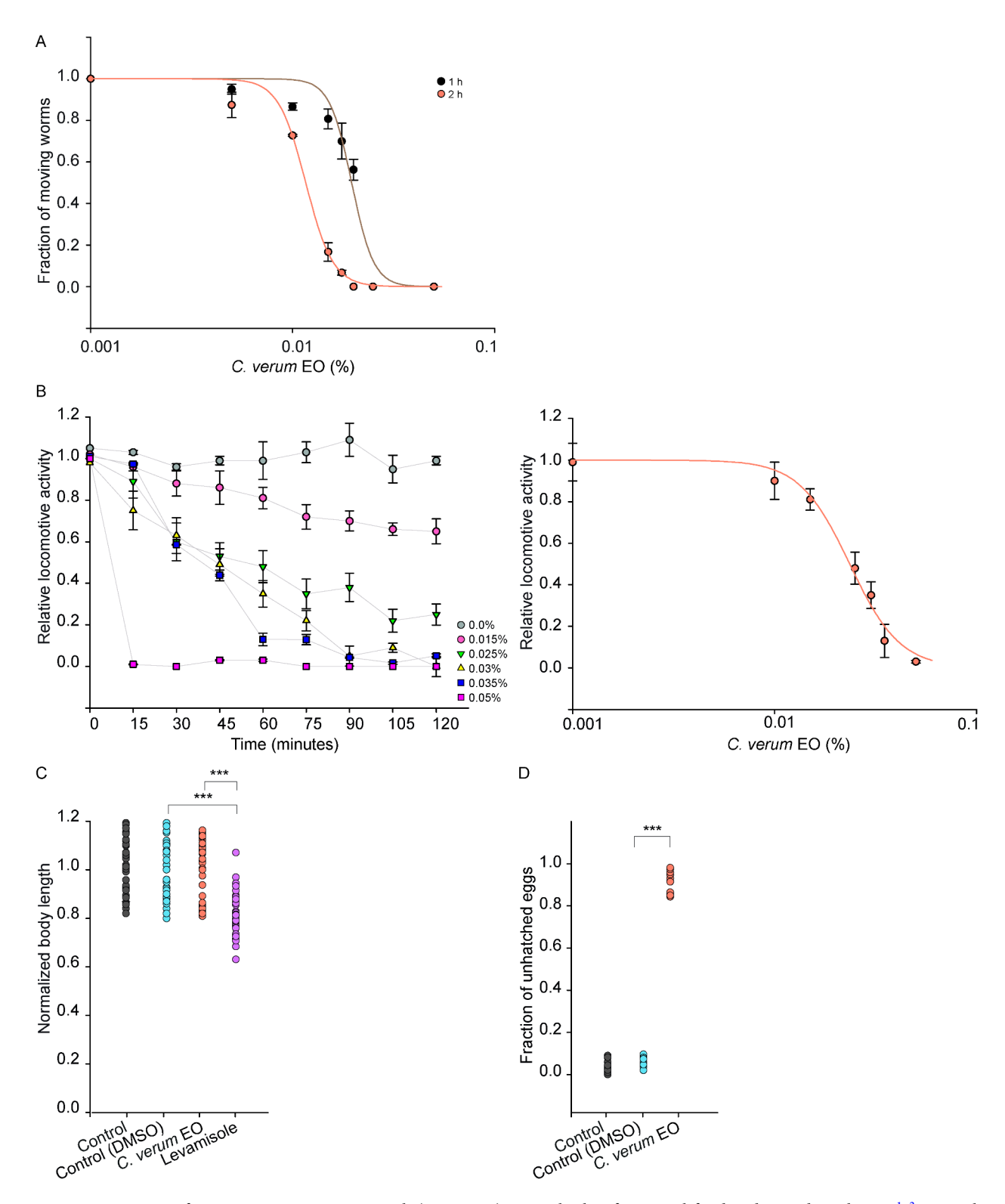
N-AChR Nicotine-sensitive ACh receptor

PZE Piperazine

TCA Trans-cinnamaldehyde

Essential oils (EO), extracted from diverse plants, are complex mixtures of natural compounds with centuriesold therapeutic applications. Recently, significant attention has been directed toward exploring the potential

Instituto de Investigaciones Bioquímicas de Bahía Blanca, Departamento de Biología, Bioquímica y Farmacia, Universidad Nacional del Sur (UNS)-CONICET, Bahía Blanca 8000, Argentina. <sup>™</sup>email: hernando@criba.edu.ar



of *Cinnamonum verum* J. Presl. (Lauraceae) EO as both a functional food and a medicinal agent<sup>1-3</sup>. Several studies underscore its antimicrobial, antibacterial, and anti-inflammatory activities, with recent investigations emphasizing its potential as eco-friendly treatment against human, veterinary, and crop pathogens<sup>4-7</sup>. Interest in *C. verum* EO is growing, particularly due to its major compound TCA, which has shown promising therapeutic benefits in both pre-clinical and clinical trials against several pathologies, such as cardiovascular diseases, Alzheimer's disease as well as bacterial, fungi and parasitic infections<sup>1,3,8</sup>. Consequently, unraveling the molecular mechanisms that drive these activities holds significant scientific interest.

Parasitic nematodes -roundworms that infect humans, animals, invertebrates and plants- cause important economic losses in livestock and crop production and contribute to neglected diseases in human and animal populations<sup>9–12</sup>. Synthetic anthelmintic drugs, which target the nervous system, locomotion, and feeding of worms, are vital for controlling infections, many of which act through Cys-loop receptors. Thus, nematode Cys-

**∢Fig. 1.** Effects of *C. verum* EO on *C. elegans.* (A) *C. verum* EO concentration-response curve for worm paralysis. The results are shown as mean  $\pm$  SD of 5 independent experiments (n = 5 agar plates with more than 30 worms per agar plate). (B) Reduction of worm locomotive activity by C. verum EO exposure. Left: Locomotive activity was recorded as a function of time in the absence or presence of C. verum EO, results are shown as mean  $\pm$  SD of 5 independent experiments (n > 12 wells per experiment, with more than 50 worms per well). Right: locomotive activity versus C. verum EO concentration for conditions as explained in left panel, constructed by measuring the reduction of activity at 1 h exposure (C) Body length measurements of C. elegans exposed 2 h to 0.025% C. verum EO, 0.1 mM levamisole, DMSO (<1%) and the respective controls without DMSO on agar plates. Each point in the plot represents the body length of an individual worm ( $n \ge 30$  worms per condition) from a representative experiment, based on three independent experiments with similar results. Measurements were normalized to the respective control condition. No statistically significant differences were detected for control plates with or without DMSO, P = 0.826 and C. verum EO vs. DMSO, P = 0.836. Normalized body length values (mean ± SD): Control: 1 ± 0.13, Control (DMSO): 1 ± 0.12, C. verum EO:  $1\pm0.139$ , levamisole:  $0.81\pm0.085$  (\*\*\*p<0.001). (D) Plot showing the ability of 0.015% C. verum EO to inhibit egg hatching following a 6-hour exposure. Each point in the plot represents the fraction of unhatched eggs per agar plate ( $n \ge 200$  eggs per plate,  $n \ge 5$  plates per condition) from a representative experiment, yielding similar results across three independent experiments. Values for the fraction of unhatched eggs per condition (mean  $\pm$  SD): control: 0.029  $\pm$  0.027; control DMSO: 0.031  $\pm$  0.026; 0.015% *C. verum* EO: 0.91  $\pm$  0.054%. \*\*\*p < 0.001.

loop receptors, crucial anthelmintic targets, are extensively studied in *Caenorhabditis elegans*, serving as models due to their resemblance to parasite receptors<sup>9,10</sup>.

Among Cys-loop receptors, the levamisole-sensitive nicotinic acetylcholine receptor (L-AChR) and the GABA-activated chloride channel (UNC-49) located in worm somatic muscle are activated by the anthelmintics levamisole and piperazine, respectively<sup>10</sup>. These receptors are crucial for coordinating worm movement and crawling. Additionally, glutamate-activated chloride channels (GluCl), which regulate neurotransmitter release and pharyngeal pumping, are activated by macrocyclic lactones like ivermectin (IVM), widely used in antiparasitic treatment<sup>13</sup>. These Cys-loop receptors are key targets in current anthelmintic therapy. However, the discovery of drugs with new mechanisms of action involving modulation rather than direct activation may offer a promising pathway to counteract the resistance that current therapies are developing.

The effectiveness of anthelmintics is threatened by limited options and emerging resistance. Synthetic drugs also pose environmental risks, highlighting the need for new natural compounds targeting different nematode targets <sup>14–16</sup>. Various EOs, including *C. verum* EO, and several bioactive molecules exhibit anthelmintic effects against parasites like *Ascaris suum*, *Parascaris* sp., *Haemonchus contortus*, *Onchocerca ochengi*, *Strongyloides ratti*, *Meloidogyne incognita*, *Bursaphelenchus xylophilus* and *Trichostrongylus* species <sup>14,17–21</sup>. However, EO face challenges in mammals due to rapid absorption and metabolism, limiting their efficacy. Future research should focus on improving bioavailability for enhanced performance <sup>22–24</sup>.

Combining classical anthelmintics with natural compounds broadens their spectrum of action by targeting multiple pathways simultaneously. This approach is effective for treating complex diseases with fewer side effects<sup>25,26</sup>. Identifying synergistic effects between bioactive molecules and commercial anthelmintics is essential for optimizing research efficiency and reducing costs.

Therefore, our study provides a detailed analysis of the anthelmintic activity of *C. verum* EO and TCA, covering aspects from the whole organism to the molecular level in *C. elegans*. This has led to the identification of TCA molecular targets and the elucidation of its mechanism of action. This comprehensive approach enhances our understanding of the anthelmintic potential of these natural compounds and supports the development of integrated therapeutic strategies.

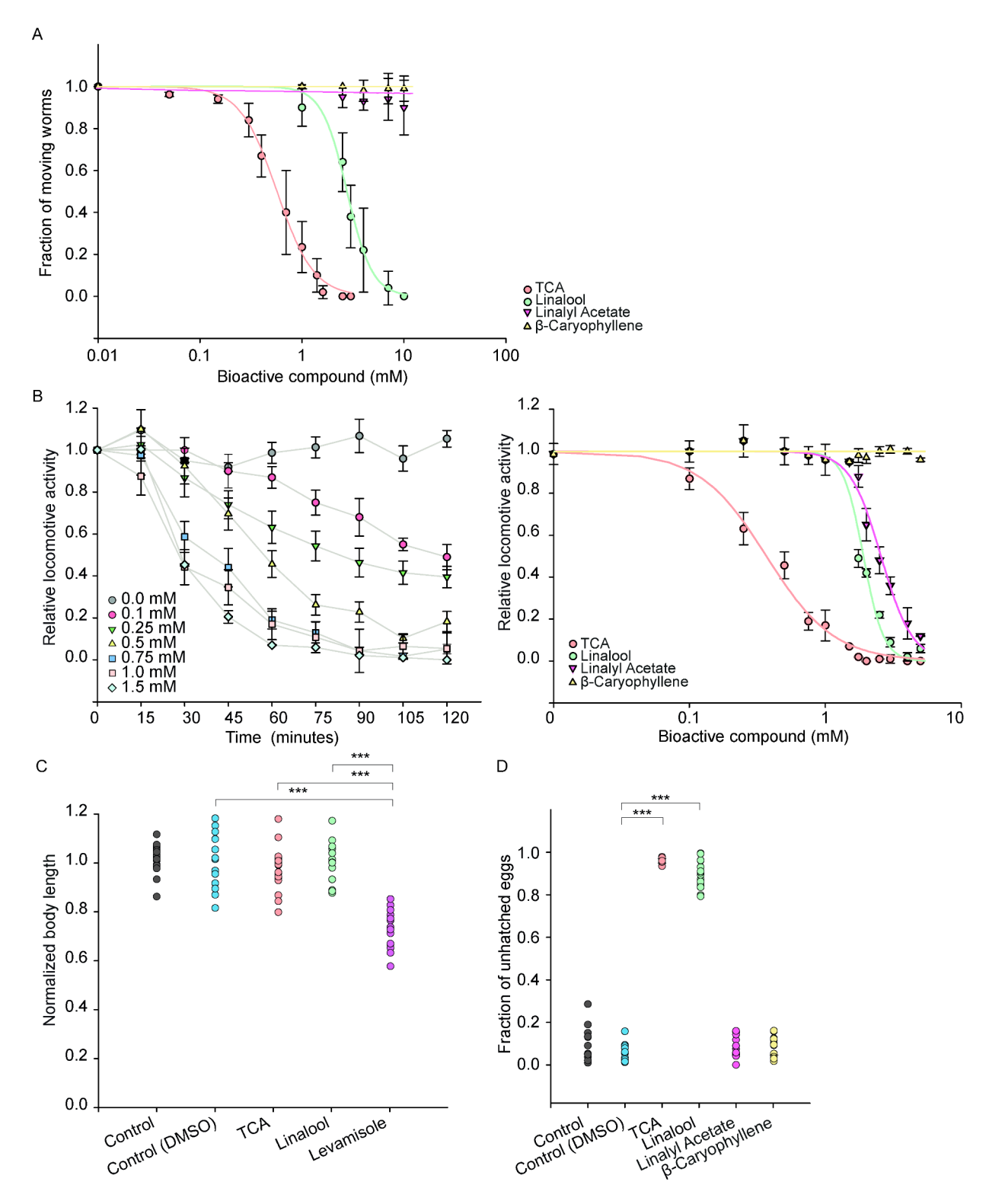
#### Results

## Inhibition of C. elegans locomotion and egg hatching by C. verum EO

Wild-type *C. elegans* worms were exposed to various concentrations of *C. verum* EO on agar plates. To measure the percentage of paralysis, we determined the fraction of worms that responded to gentle touch (moving worms) after 1 and 2 h. The results showed that *C. verum* EO effectively inhibited worms' locomotion, with an IC50 value of  $0.02\pm0.001\%$  and  $0.0116\pm0.0012\%$  (v/v) after 1 and 2 h exposure, respectively (Fig. 1A). This inhibitory effect was time-dependent, as greater locomotion inhibition was observed after 2 h of exposure, demonstrating enhanced impact with prolonged treatment.

Given that neural mechanisms for swimming are different from those for crawling, we further evaluated the effect of *C. verum* EO as a function of time and concentration on adult worms using an automated thrashing assay in liquid medium (Fig. 1B). After 1 h exposure, *C. verum* EO (0.005–0.05%) affected locomotor activity of wild-type worms, yielding an IC50 value of 0.024±0.001% (Fig. 1B). In contrast, the motility of the control group in the absence of the *C. verum* EO remained stable for the 2 h-period.

Detailed analysis of paralysis features and body length measurements on agar plates indicated that C. verum EO induced paralysis of body wall muscles, along with the suppression of head and tail movements, without altering the normal length of the worms. Measurement of worms treated 2 h with 0.025% C. verum EO did not exhibit significant differences compared to the control (Fig. 1C). As a control for spastic paralysis, the anthelmintic levamisole was used as it reduces worm length by acting as an agonist of L-AChR (Fig. 1C). In the presence of levamisole, a statistically significant difference in worm length compared to the drug-free control was observed (p<0.01).



In our pursuit to investigate whether *C. verum* EO exerts direct influence on egg hatching, we performed the egg hatching assay following our established protocol<sup>27</sup>. Remarkably, *C. verum* EO produced a marked inhibition of egg hatching. At 0.015%, the fraction of unhatched eggs was  $0.91\pm0.054\%$  (Fig. 1D). Higher concentrations further enhanced the inhibition, reaching  $0.98\pm0.026\%$  at 0.0175% and  $100\pm0\%$  at 0.02%. These findings indicate that *C. verum* EO exerts a direct negative impact on egg hatching, correlating with prolonged anthelmintic effects.

**∢Fig. 2.** Action of bioactive molecules from *C. verum* EO on *C. elegans* (A) Concentration-response curves for worm paralysis. Wild-type worms were exposed 2 h to TCA, linalool, linalyl acetate or  $\beta$ -caryophyllene at different concentrations. The results are shown as mean ± SD of at least 5 independent experiments for each condition (n = 5 agar plates per condition per experiment, with more than 30 worms per agar plate). (B) Analysis of worm locomotive activity over time and in response to varying concentrations of bioactive molecules. Left: Locomotive activity was monitored over time in the absence or presence of TCA. Results are shown as mean  $\pm$  SD of 5 independent experiments (n > 12 wells per experiment, with more than 50 worms per well). Right: Concentration-dependent reduction in locomotive activity, plotted as a function of TCA concentration, based on activity measured after 1 h of exposure. (C) Plot showing the normalized body length of wild-type worms under different conditions. Each point in the plot represents the body length of an individual worm ( $n \ge 30$  worms per condition) from a representative experiment, based on three independent experiments with similar results. Normalized body length values (mean ± SD): Control: 1±0.11; Control (1% DMSO): 0.99±0.125 (1% DMSO did not induce statistically significant changes in body length compared to the control group without DMSO (P=0.826)); 0.5 mM TCA: 1.05 ± 0.13; 6 mM linalool: 0.98 ± 0.11; and 0.1 mM levamisole: 0.74 ± 0.04. Statistical analysis revealed no significant differences between controls and treatments (p>0.1) except for levamisole, which significantly reduced body length (p < 0.001 for all comparisons) (D) Plot showing the ability of 0.5 mM TCA and 6 mM linalool to inhibit egg hatching after a 6-hour exposure. Results are presented as the fraction of unhatched eggs under the specified conditions; each data point represents an agar plate containing over 200 eggs ( $n \ge 5$  agar plate per condition) from a representative experiment, yielding similar results across three independent experiments. Values for the fraction of unhatched eggs per condition (mean ± SD): control: 0.1106 ± 0.0802; control DMSO:  $0.0763 \pm 0.0493$ ; TCA:  $0.9545 \pm 0.0163$ ; linalool:  $0.8789 \pm 0.0793$ ; linalyl acetate:  $0.085 \pm 0.0563$ ;  $\beta$ -caryophyllene: 0.0864 ± 0.0573. No statistically significant differences were found between controls with or without DMSO (P=0.104). \*\*\*p < 0.001.

## Profiling of EO composition and search for active compounds involved in the inhibition of *C. elegans* locomotion

Several studies have compiled information regarding the composition of *C. verum* EO, emphasizing its variations not only depending on the cinnamon species but also on specific plant parts and seasonal factors, among other variables<sup>28</sup>.

The primary components found in the *C. verum* EO, namely trans-cinnamaldehyde (TCA, phenylpropene aldehyde-type), linalool (a monoterpene), linalyl acetate (an acetate ester of linalool), and  $\beta$ -caryophyllene (a bicyclic sesquiterpene), comprise approximately 90% of the oil's total composition (Table S1). A qualitative analysis of the *C. verum* EO utilized in our experiments was conducted using GC-MS, and the compounds detected are detailed in Table S2. The results of the composition of our *C. verum* EO demonstrated consistency with previous reports and confirmed the presence of TCA, which constitutes the major component in all EO samples ( $\geq 60\%$  TCA)<sup>28</sup>.

We selected TCA and three other compounds, linalool, linalyl acetate and  $\beta$ -caryophyllene, also reported to be present in *C. verum* EO samples, due to their diverse chemical structures for further exploring their effects on *C. elegans*. The primary objective was to identify the main contributors to the observed anthelmintic activity.

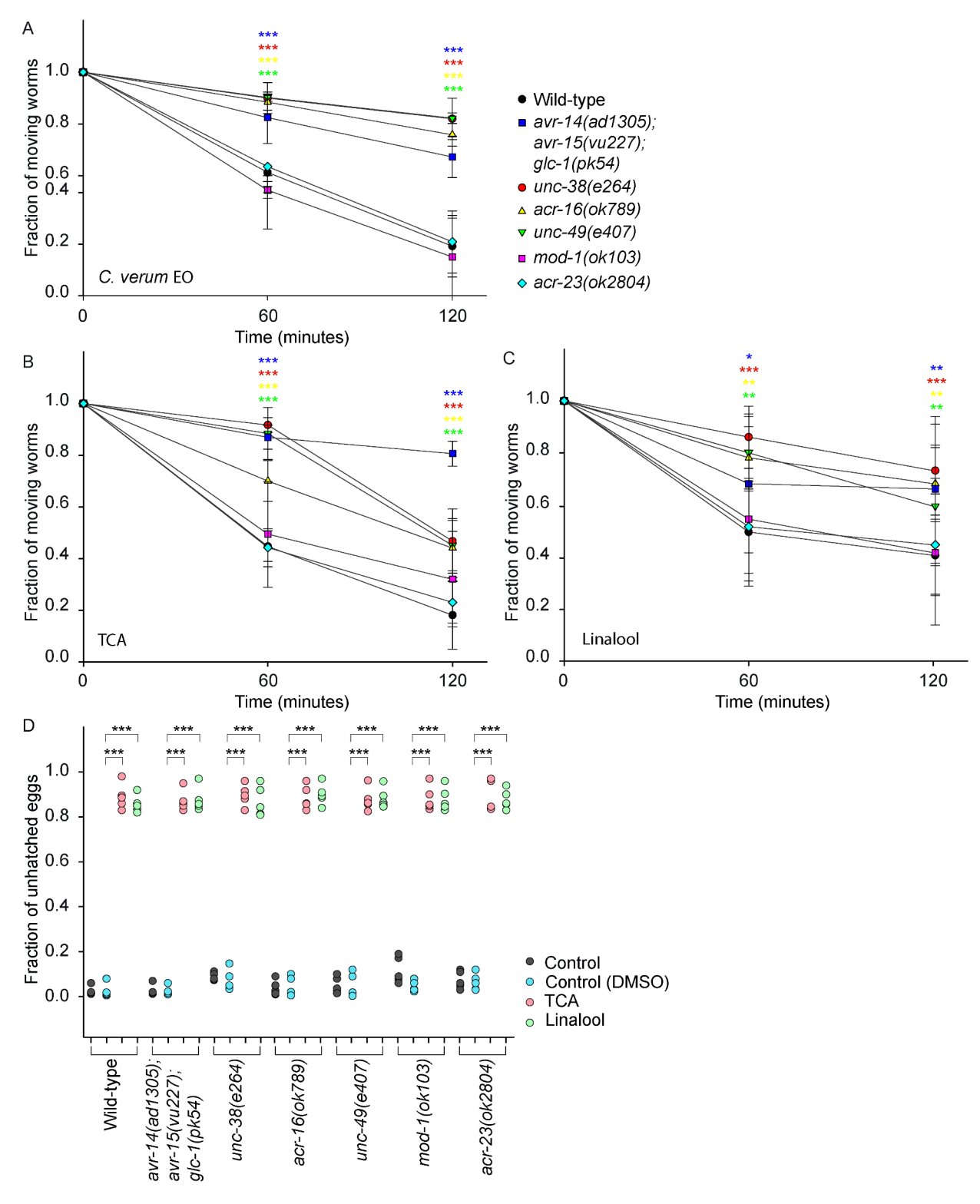
The assessment of the effects of these compounds on wild-type C. elegans worms on agar plates resulted in IC50 values of  $0.56\pm0.04$  mM for TCA and  $2.76\pm0.082$  mM for linalool following a 2-hour exposure. Remarkably, no paralysis was observed for linalyl acetate and  $\beta$ -caryophyllene, even at concentrations as high as 10 mM (Fig. 2A). We also assessed the changes in adult worms' locomotive activity due to the exposure to TCA as a function of time (Fig. 2B, left panel), and to TCA, linalool, linalyl acetate, and  $\beta$ -caryophyllene at a range of concentrations (Fig. 2B, right panel) using an automated thrashing assay in liquid medium. The compounds affected wild-type worms' locomotor activity, with TCA showing the highest potency; IC50 values as follows:  $0.368\pm0.02$  mM TCA>1.9026 $\pm0.0535$  mM linalool>2.5626 $\pm0.0658$  mM linalyl acetate (Fig. 2B). Linalyl acetate, but not  $\beta$ -caryophyllene, was capable of reducing locomotive activity of wild-type worms. These findings propose TCA as a key bioactive molecule present in C. Verum EO.

While previous studies have reported C. elegans motility inhibition in liquid medium caused by prolonged exposure to TCA at high concentrations<sup>29–31</sup>, the detailed characteristics of the paralysis have not been described. Thus, we measured body length of C. elegans as described for C. verum EO. No statistical differences were found in the measurement of the mean worm body length calculated for the condition with 0.5 mM TCA and 2.5 mM linalool compared to the control condition (Fig. 2C). The results for egg hatching assay showed that 0.5 mM TCA and 6 mM linalool were capable of inhibiting egg hatching reaching values close to 90%, whereas 10 mM linalyl acetate and 10 mM  $\beta$ -caryophyllene did not demonstrate such effects (Fig. 2D), consistent with the lack of effects found in the paralysis assays.

In summary, we showed that TCA, which induces rapid paralysis and significant egg hatching inhibition, is a key bioactive molecule of *C. verum* EO associated with its anthelmintic effect. While linalool also exhibited anthelmintic activity, it was less potent than TCA, reinforcing the idea that TCA is a main contributor to the *C. verum* EO effects.

#### C. verum EO, TCA and linalool act through multiple targets in C. elegans

The identification of the molecular targets is a crucial step in drug discovery, as it helps to understand how a compound exerts its biological effects. By using mutant strains, we explored if several Cys-loop receptors, which belong to the family of pentameric-ligand gated ion channels, are involved in the paralyzing effects of



EO and its main components. The tested receptors include the glutamate-activated chloride channel (GluCl), two nicotinic acetylcholine receptors (L-AChR and N-AChR), the GABA-activated chloride channel (UNC-49), the serotonin-activated chloride channel (MOD-1), and the betaine-activated ion channel (ACR-23)<sup>32</sup>. These receptors play key roles in nematode motility and most of them are targets of classical anthelmintic agents<sup>10</sup>.

To assess the contribution of GluCls, we utilized the triple null mutant strain, avr-14(ad1305);avr-15(vu227);glc-1(pk54), which is resistant to IVM. Following 1 and 2-h exposure period to 0.02% C. verum EO, 0.5 mM TCA and 2.8 mM linalool on agar plates (Fig. 3A, B and C, respectively), the fraction of moving mutant worms was significantly higher compared to wild-type worms. This indicates that specific subtypes of GluCls play a role in the paralysis induced by C. verum EO, TCA and linalool.

We also performed paralysis assays on agar plates with mutant strains lacking Cys-loop receptors located in somatic muscle: the *unc-38(e264)* strain lacking the L-AChR, the *acr-16(ok789)* strain lacking the N-AChR, and

**∢Fig. 3.** Deciphering molecular targets mediating 0.02% *C. verum* EO (A), 0.5 mM TCA (B) and 2.8 mM linalool (C) effects by using C. elegans mutant strains. Each point represents the mean ± SD of the fraction of moving worms ( $n \ge 30$  worms per agar plate, with 5 agar plates per strain in each experiment) from a representative whole experiment. Three independent experiments per strain were carried out yielding similar results. Wild-type strain compared to mutant strains: avr-14(ad1305);avr-15(vu227);glc-1(pk54), unc-38(e264), acr-16(ok789), unc-49(e407), mod-1(ok103) and acr-23(ok2804). The color-coding of the mutant strains, introduced in panel (A), applies to all panels (B) and (C) as well. Mutant strains that did not differ significantly from the wild-type strain showed p > 0.1, while significant differences are marked with asterisks, \*p < 0.05, \*\*p < 0.01 and \*\*\*p < 0.001. Asterisks are color-coded to correspond with each mutant strain, matching the colors used to represent their data points in the figure. (D) Plot showing the ability of 0.5 mM TCA or 6 mM linalool to inhibit egg hatching in wild-type and mutant strains of C. elegans after a 6-hour exposure. Each point in the plot corresponds to the fraction of unhatched eggs per agar plate ( $n \ge 200$  eggs per agar plate,  $n \ge 5$  plates per condition) from a representative experiment, yielding similar results across three independent experiments. Values for the fraction of unhatched eggs per strain are presented in Table S3. A significant reduction in egg hatching is observed in the presence of TCA and linalool compared to the control group. \*\*\*p < 0.001.

the *unc-49(e407)* strain lacking functional UNC-49 receptor. All mutant strains exhibited partial resistance to *C. verum*, TCA and linalool (Fig. 3A, B and C, respectively). Nevertheless, at concentrations higher than the IC50 values (0.03% for *C. verum* EO and 1 mM for TCA), all tested mutant worms responded similar to the wild-type, indicating that the partial resistance to *C. verum* EO and TCA is overcome by higher concentrations.

The mod-1(ok103) strain lacks the serotonin (5-HT)-activated chloride channel MOD-1, identified as a potential anthelmintic target, and the acr-23(ok2804) mutant strain lacks ACR-23, a crucial target for monepantel (MNP) anthelmintic effect<sup>10</sup>. Both mutant strains did not show statistically significant differences in the fraction of moving worms on agar plates compared to wild-type worms when exposed to C. verum EO, TCA or linalool, suggesting that these receptors are not major contributors to the paralysis (Fig. 3A, B and C, respectively).

With the aim of further exploring the role of TCA and linalool as anthelmintic compounds and their potential to reduce egg hatching in resistant nematodes, we also assessed the ability of TCA and linalool to inhibit egg hatching in both wild-type and mutant strains. Our results demonstrate that both bioactive molecules effectively reduce egg hatching in all tested strains, with similar effects observed in both wild-type and mutant strains (Fig. 3D and Table S3).

In summary, our study using mutant strains identifies several key molecular targets for worm paralysis induced by *C. verum* EO. It is important to note that while we propose that GluCl, L-AChR, N-AChR, and UNC-49 contribute to the paralyzing effects of *C. verum* EO, TCA, and linalool, other potential targets—beyond those examined in this study—cannot be ruled out.

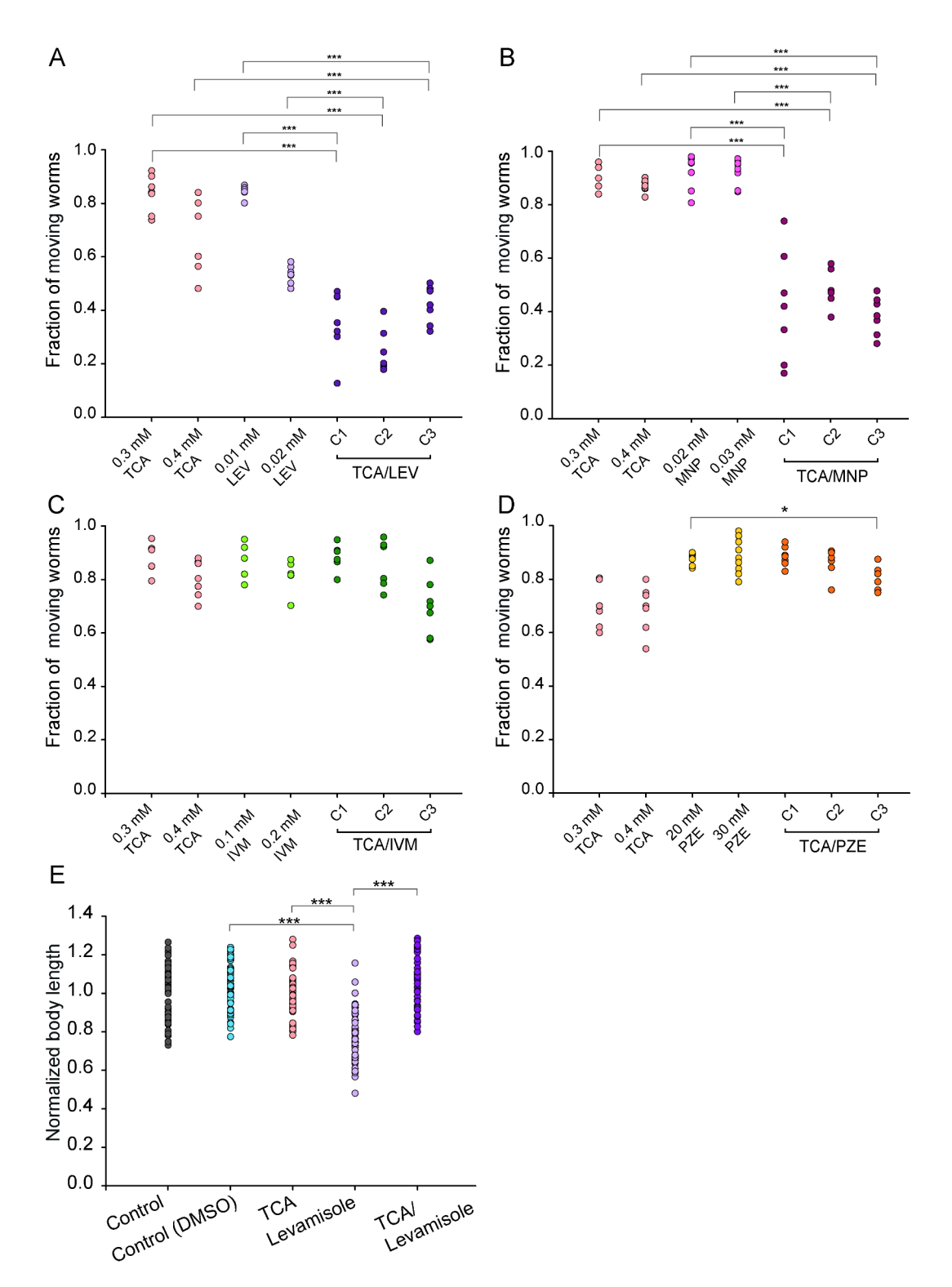
#### Exploring combinations of TCA with classical anthelmintic drugs for enhanced efficacy

We selected for the drug combination assay the classical anthelmintics levamisole (LEV), monepantel (MNP), ivermectin (IVM) and piperazine (PZE), all acting through different Cys-loop receptors<sup>10</sup>. The novel compound chosen as the reference drug was TCA.

For the combination TCA/LEV, we tested concentrations of TCA (0.05 mM-1.4 mM) and LEV (0.005 mM-0.06 mM) alone and the combinations namely C1: 0.3 mM TCA+0.01 mM LEV; C2: 0.3 mM TCA+0.02 mM LEV and C3: 0.4 mM TCA+0.01 mM LEV (Fig. 4A and S1A Fig.). The results revealed a higher paralyzing effect for each respective combination of TCA/LEV compared to the sum of each drug alone at the same concentration, indicating a synergistic effect. In the combination TCA/MNP, the tested concentrations were MNP (0.02 mM-1 mM); C1: 0.3 mM TCA+0.02mM MNP; C2: 0.3 mM TCA+0.03 mM MNP and C3: 0.4 mM TCA+0.02 mM MNP. The TCA/MNP combination exhibited a greater paralyzing effect compared to the sum of each drug alone, also suggesting a synergistic effect (Fig. 4B and Fig. S1B). In contrast, the results from the combinations of TCA (0.05 mM-1.4 mM) with IVM (0.05-0.4 mM) or PZE (10-45 mM) showed no relevant changes in paralyzing effect compared to each drug alone (Fig. 4C and D and Fig. S1C and S1D, respectively). This highlights the importance of identifying ineffective drug combinations in preclinical stages to optimize the development of therapeutic strategies.

To provide a more accurate assessment of the effect resulting from the drug combination, we calculated the CI values using Chou-Talalay's CI theorem. The resulting CI values were < 0.85 for both TCA/LEV and TCA/MNP combinations; C1: 0.65, C2: 0.75 and C3: 0.58 for TCA/LEV, and C1: 0.58, C2: 0.52 and C3: 0.62 for the TCA/MNP, indicating a synergistic effect and valuable benefits of drug combination. In contrast, the CI values were > 1.45 for TCA/IVM and for TCA/PZE (TCA/IVM C1: 4.25, C2: 4.05 and C3: 1.61 and TCA/PZE C1: 5, C2: 4.4 and C3: 3.4), indicating antagonistic action when the drugs are combined.

To gain deeper insights into the interaction between TCA and LEV, both of which paralyze the worms, we explored the effect of their combination on worm body length. While levamisole, an agonist of L-AChRs, reduced the body length, TCA alone did not affect body length, suggesting it does not directly activate L-AChRs. The combination of TCA and LEV showed that TCA significantly reduced the levamisole-induced contraction in body length of C. elegans (Fig. 4E; p < 0.001). These findings distinguish the effects of TCA from those of classical agonists.



## Modulation of cys-loop receptors by TCA: macroscopic currents of L-AChR and UNC-49 are inhibited by TCA

To elucidate the molecular mechanism underlying the anthelmintic effects of TCA, we performed electrophysiological studies of candidate receptors identified from paralysis assays in mutant worms.

To determine if TCA acts through L-AChR and UNC-49, we first recorded macroscopic currents of native receptors from cultured L1 muscle cells elicited by 1 mM ACh or 1 mM GABA, respectively (holding potential: -70 mV). Whole-cell current features of both L-AChR and UNC-49 receptors at L1 muscle cells have been described in previous studies  $^{10}$ . Pre-exposure of L1 cells to 0.1 mM TCA for 1 min resulted in a statistically significant decrease of the peak currents elicited by ACh or GABA to  $75\pm15\%$  and  $73\pm16\%$ , respectively (n=10 and n=9 cells per condition, respectively, Fig. 5A and B). Control currents treated with DMSO alone did not exhibit statistically significant reductions in peak currents ( $94\pm8\%$  peak current relative to the control). After a 1-min wash with ECS solution, the control peak currents were restored ( $84\pm17\%$  and  $87\pm16\%$ , respectively, of

**∢Fig. 4**. Exploring drug combinations with TCA for anthelmintic treatment. Plot showing the fraction of moving worms after 1 h-exposure on agar plates to TCA, anthelmintic and TCA/anthelmintic combination. Each point represents the fraction of moving worms per agar plate ( $n \ge 30$  worms per agar plate, with 5–9 agar plates per condition) from a representative experiment, shown for each panel. (A) TCA, levamisole (LEV) and TCA+LEV combos, C1: 0.3 mM TCA+0.01 mM LEV; C2: 0.3 mM TCA+0.02 mM LEV and C3: 0.4 mM TCA + 0.01 mM LEV. Values for each condition (mean ± SD): 0.3 mM TCA: 83.43 ± 7.63; 0.4 mM TCA:  $67.19 \pm 14.44$ ; 0.01 mM LEV:  $84.23 \pm 2.31$ ; 0.02 mM LEV:  $53.17 \pm 3.71$ ; C1:  $35.20 \pm 13.25$ ; C2:  $24.20 \pm 9.03$ ; C3: 41.83 ± 7.65. (B) TCA, monepantel (MNP) and TCA + MNP combos, C1: 0.3 mM TCA + 0.02 mM MNP; C2: 0.3 mM TCA + 0.03 mM MNP and C3: 0.4 mM TCA + 0.02 mM MNP. Values for each condition (mean ± SD): 0.3~mM TCA:  $90.83 \pm 4.67$ ; 0.4~mM TCA:  $87.17 \pm 2.61$ ; 0.02~mM MNP:  $92.12 \pm 7.27$ ; 0.03~mM MNP: 93.34 ± 5.03; C1: 42.01 ± 22.70; C2: 47.17 ± 8.59; C3: 38.57 ± 7.77. (C) TCA, ivermectin (IVM) and TCA + IVM combos, C1: 0.3 mM TCA + 0.2 mM IVM; C2: 0.3 mM TCA + 0.3 mM IVM and C3: 0.4 mM TCA + 0.2 mM IVM. Values for each condition (mean ± SD): 0.3 mM TCA: 87.92 ± 5.80; 0.4 mM TCA: 80.40 ± 7.52; 0.2 mM IVM:  $85.50 \pm 7.26$ ; 0.3 mM IVM:  $81.49 \pm 6.01$ ; C1:  $88.42 \pm 5.04$ ; C2:  $85.71 \pm 9.06$ ; C3:  $70.05 \pm 11.55$ . (D) TCA, piperazine (PZE) and TCA + PZE combos, C1: 0.3 mM TCA + 20 mM PZE; C2: 0.3 mM TCA + 20 mM PZE and C3: 0.4 mM TCA + 20 mM PZE. Values for each condition (mean ± SD): 0.3 mM TCA: 70.12 ± 8.66; 0.4  $mM\ TCA: 69.17 \pm 9.56; 20\ mM\ PZE: 87.60 \pm 2.42; 30\ mM\ PZE: 89.05 \pm 5.68; C1: 88.5 \pm 4.04; C2: 85.99 \pm 5.39; 20.00 \pm 1.00 \pm 1.00 \pm 1.00$ C3: 80.48 ± 4.73. Four independent experiments were carried out yielding similar results. Comparisons that did not differ significantly showed p > 0.1, while significant differences are marked with asterisks, \* p < 0.05and \*\*\*p < 0.001. (E) Plot showing the changes in body length of wild-type worms exposed to DMSO (1%), 0.5 mM TCA, 0.1 mM levamisole, and the combination of 0.5 mM TCA + 0.1 mM levamisole. Each point in the plot represents the body length of an individual worm ( $n \ge 30$  worms per condition) from a representative experiment, yielding similar results across three independent experiments. Normalized body length values (mean  $\pm$  SD): control:  $1\pm0.14$ ; control (1% DMSO):  $1.04\pm0.12$ ; TCA:  $0.997\pm0.117$ ; LEV:  $0.789\pm0.13$ ; TCA/ LEV: 1.05 ± 0.13. Statistical analysis revealed no significant differences between controls and treatments (p>0.1) except for levamisole, which significantly reduced body length (p<0.001 for all comparisons). \*\*\*p < 0.001.

the original currents measured in the same cell). Higher TCA concentrations (> 0.5 mM) resulted in membrane instability and could not be examined.

Additionally, the application of 0.1 mM TCA to cells expressing the receptor under study, in the absence of agonists, did not generate macroscopic responses, indicating that it is not an agonist of these receptors (Table S4).

Since  $GluCl\alpha 1/\beta$  heteropentamers have been previously expressed and electrophysiologically characterized in BOSC-23 cells<sup>33</sup>, we used this system to measure macroscopic currents elicited by 3–5 mM glutamate in the whole-cell configuration. Macroscopic currents of  $GluCl\alpha 1/\beta$  induced by 3 mM and 5 mM glutamate were not affected by 60–90 s pre-incubation with 0.1 mM TCA (n=8 and n=5, respectively, Fig. 5C). No statistically significant differences in peak currents were detected compared to the control pre-incubated with DMSO alone (Fig. 5C). Increasing both the concentration of TCA (to 0.5 mM) and the time of pre-incubation (to 120 s) did not result in any significant change in the glutamate-elicited currents. Additionally, TCA was incapable of generating currents by itself in the absence of the agonist (Table S4). Thus, this GluCl subtype does not appear to be involved in the reduced sensitivity of the triple mutant worms to TCA, suggesting that other unexplored GluCl subtypes may contribute to the paralyzing activity of TCA.

We expressed MOD-1 in BOSC-23 cells and measured macroscopic currents elicited by rapid application of 1  $\mu$ M 5-HT<sup>34</sup>. After a 60–90 s preincubation period with 0.1 mM TCA, no changes in the peak currents compared to the control currents were observed (n = 5, Fig. 5D). In addition, TCA failed to generate currents in the absence of an agonist (Table S4). These results support the findings from paralysis assays conducted on the mutant strain lacking MOD-1, which showed no difference compared to the wild-type strain and exhibited no resistance to TCA.

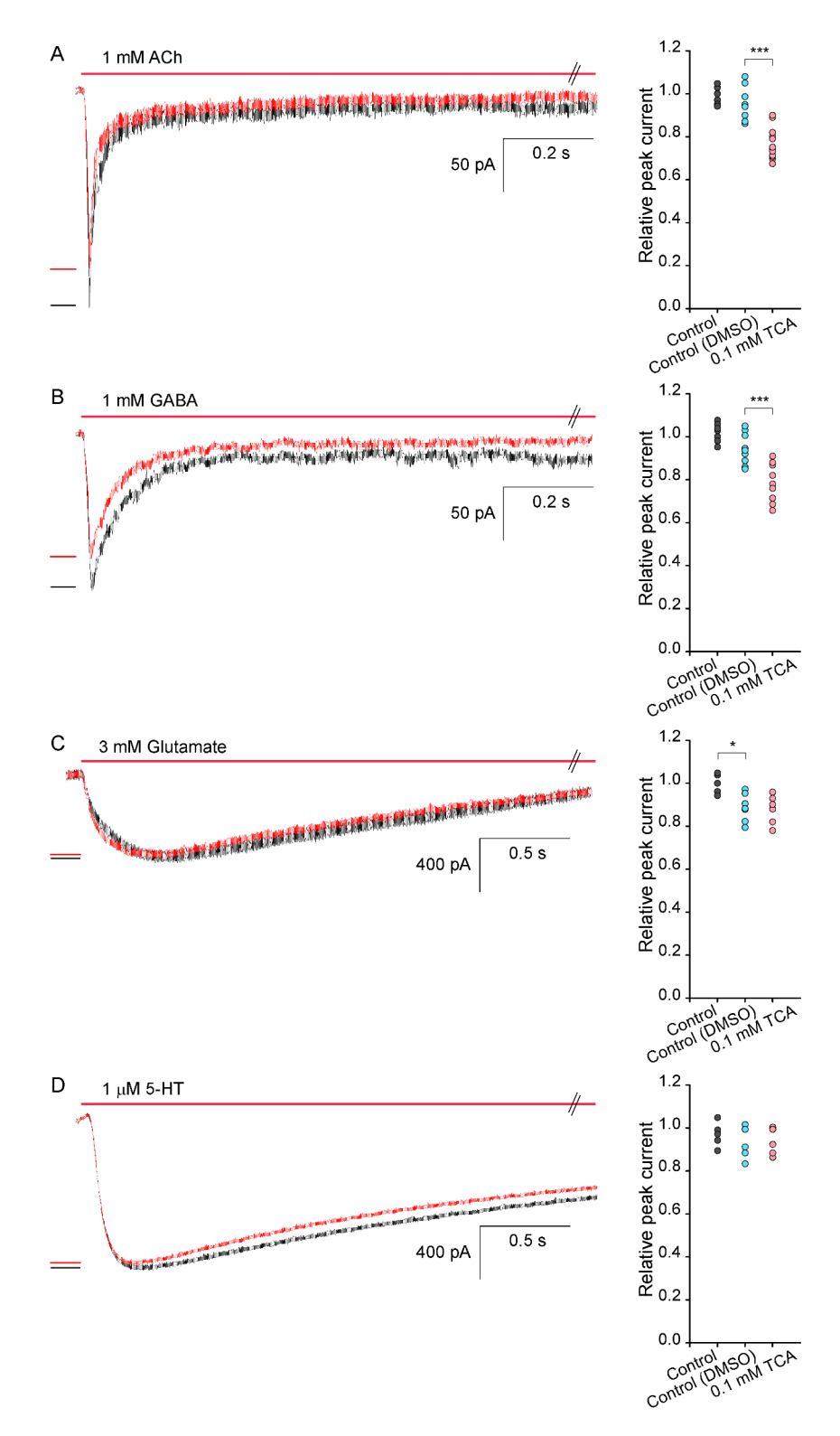
In summary, our whole cell analysis demonstrated that TCA modulates L-AChR and GABA receptors by reducing the peak currents, indicating that it acts as an inhibitor of these receptors. This finding provides insights into how TCA may exert its anthelmintic effects.

#### Effects of TCA on L-AChRs single-channel activity elicited by ACh and levamisole

To gain further insights into the molecular actions of TCA and to unravel its modulation of native L-AChR, we recorded single-channel currents activated by ACh or levamisole in the cell-attached configuration from L1 muscle cells. Recordings of channel activity at 100  $\mu$ M ACh revealed the presence of openings with an amplitude of 3.5  $\pm$  0.38 pA (n=10) at a holding potential of 100 mV, which is consistent with previous reports<sup>35,36</sup>. As a control, we verified that 0.02% DMSO did not produce any change in the single-channel activity pattern and channel properties (n=5).

To assess the effects of TCA, L1 cultured cells were incubated for 15–20 min with 0.02% DMSO with or without  $100\,\mu\text{M}$  TCA, and single L-AChR currents activated by ACh were recorded as described above (Fig. 6A). In the control condition, the frequency of openings remained mainly constant during the recording, exhibiting few long silent periods. In contrast, the long silent periods were more frequent in the presence of TCA (Fig. 6A).

Open time histograms for 100  $\mu$ M ACh+100  $\mu$ M TCA were fitted by one exponential component, with a mean open duration significantly reduced compared to the control condition (0.12±0.013 ms and 0.23±0.04 ms, respectively, Fig. 6B; Table 1). Closed-time distributions of L-AChRs from both conditions were described



by the sum of three or four components. The main closed component, about 32 ms, was displaced to smaller durations in recordings from cells treated with TCA (Fig. 6B; Table 1).

At a lower TCA concentration (1  $\mu$ M), openings elicited by 100  $\mu$ M ACh were also briefer than the control (0.12  $\pm$  0.02 ms, Table 1). Also, a higher frequency of long closed periods was observed in cells treated with 1  $\mu$ M TCA compared to the control (Fig. 6A).

The duration and number of the prolonged silent periods was variable among different recordings since it also depends on the number of receptors in the patch. To quantify, we measured only the silent periods longer than 0.5 s in the whole recording and calculated the percentage of time in which the channel is in these long-closed states, relative to the total recording time. Although the percentages corresponding to silent periods were variable, a systematic increase with TCA concentration was detected. The percentage for the control condition of channels activated by  $100 \, \mu M$  ACh was  $9 \pm 12\%$  (n = 10), which is statistically significantly different to  $29 \pm 14\%$ 

∢Fig. 5. Inhibitory effects of TCA on L-AChR and UNC-49 macroscopic currents. Left: Typical whole-cell traces from *C. elegans* L1 cultured muscle cells elicited by a 1 s-pulse of ACh (A) or GABA (B) before (DMSO control current, black traces) and after 1 min incubation period with 0.1 mM TCA (treated current, red traces); pipette potential: -70 mV. Macroscopic responses of GluClα1/β elicited by 3 mM glutamate (C) and MOD-1 elicited by 1 μM 5-HT (D); pipette potential: -50 mV. For all panels, cells were first exposed to a pulse of agonist in ECS (normalized current to 1), then to a 1 min pulse ECS alone (DMSO control) or 0.1 mM TCA incubation period, and finally again to the agonist (DMSO control: black traces; treated current: red traces). The red upper line shows the time of exposure to the agonist. For clarity, the maximal peaks are indicated by black (DMSO control) and red (TCA treatment) lines at the left. Right: plot showing the relative peak current for TCA treated currents compared to its DMSO control. Each point represents the average current for a single cell. Values for the right panels in each condition (mean ± SD): (A) control: 1 ± 0.07; control DMSO: 0.96 ± 0.1; 0.1 mM TCA: 0.75 ± 0.15. (B) control: 1 ± 0.066; control DMSO: 0.945 ± 0.12; 0.1 mM TCA: 0.73 ± 0.16. (C) control: 1 ± 0.08; control DMSO: 0.89 ± 0.1; 0.1 mM TCA: 0.88 ± 0.11. (D) control: 1 ± 0.08; control DMSO: 0.967 ± 0.1; 0.1 mM TCA: 0.978 ± 0.09. \*\*\*p < 0.001.

(n=10, P=0.048) and  $37\pm26\%$  (n=11, P=0.004) for 100  $\mu$ M ACh in combination with 1 or 100  $\mu$ M TCA, respectively.

We also thoroughly explored recordings in the presence of a lower ACh concentration,  $10~\mu M$  ACh, in the absence and presence of  $100~\mu M$  TCA. At  $10~\mu M$  ACh, open time histograms were described by one exponential component whose duration was longer than that detected for  $10~\mu M$  ACh +  $100~\mu M$  TCA ( $0.29\pm0.01$  ms and  $0.16\pm0.03$  ms, respectively, Table 1). Also, the percentage of the silent periods was higher when TCA was present ( $19\pm9\%$  for ACh alone and  $42\pm19\%$  for  $10~\mu M$  ACh and  $100~\mu M$  TCA, P=0.047).

To expand the analysis, we recorded single channel events evoked by 100  $\mu$ M LEV alone and in combination with 100  $\mu$ M TCA (Fig. 6C). Open time histograms were fitted by one exponential component whose duration was reduced compared to that detected in the control condition (0.13  $\pm$  0.03 ms and 0.27  $\pm$  0.04 ms, respectively, Table 1). We also observed long silent periods in the presence of TCA, whose durations were also variable between recordings. However, the percentage of the time in these long silent periods was statistically significantly different to the control, 45  $\pm$  21% (n = 6) for 100  $\mu$ M LEV alone (control) and 78  $\pm$  20% (n = 6, P = 0.021) for 100  $\mu$ M LEV in combination with 100  $\mu$ M TCA.

To extend the analysis even more, we examined the duration of bursts, which correspond to the activation episode of a single receptor molecule. We found that the mean burst durations were significantly briefer in the presence of TCA compared to control conditions (p<0.05; Table 1). These results highlight TCA's inhibitory effect on receptor activation, providing additional insights into its mechanism of action.

In conclusion, TCA inhibits single-channel activity of L-AChR by increasing the proportion of long electrically silent periods in which the receptor is not active and reducing the open and burst durations.

#### Discussion

In this study, we focus on identifying the molecular targets and mechanisms of action of TCA from *C. verum* EO, examining its effects on the nematode model *C. elegans* from organismal to molecular levels. Although research on the effects of essential oils on parasitic nematodes remains limited<sup>16,17,22</sup>, our research confirms TCA and linalool as key components contributing to the anthelmintic activity of *C. verum* EO and builds upon and extends the understanding provided by earlier studies on TCA's anthelmintic potential<sup>29–31</sup>. Through TCA screening of mutant worms, our results reveal that several Cys-loop receptors, including L-AChR, N-AChR, UNC-49 and GluCl receptors, contribute as novel targets to its anthelmintic activity (Fig. 7). Our electrophysiological recordings demonstrate that TCA reduces macroscopic responses of L-AChR and UNC-49 receptors, indicating its inhibitory action. Additionally, single channel recordings of L-AChR demonstrate that TCA decreases the frequency and the duration of L-AChR channels, a change consistent with noncompetitive inhibition, suggesting a distinct mechanism to the classical anthelmintics<sup>37</sup>.

While the participation of GluCl receptors in the anthelmintic activity elicited by TCA has been suggested through the screening of mutant worms, direct electrophysiological evidence supporting their involvement remains to be elucidated, underscoring the need for further investigation.

Moreover, our study explores the synergistic potential of TCA when combined with conventional anthelmintics, offering insights into future formulations aimed at mitigating resistance acquisition and enhancing treatment efficacy. The strategy of using multitarget-directed ligands that simultaneously affect various Cys-loop receptors crucial for worm function offers potential for advancing the development of anthelmintic therapies.

The anthelmintic activity of C. verum EO is evident through various experimental assays that revealed worm paralysis on agar plates, reduced locomotor activity in liquid medium, and significant inhibition of egg hatching. These assays cover various aspects of worm physiology and illustrate effects across different timeframes, from immediate changes in locomotion to sustained anthelmintic impact by preventing egg hatching. TCA has been shown to constitute more than 50% of the components of a great variety of C. verum samples (see Table S1). We confirmed the presence of TCA in our C. verum EO sample by a qualitative analysis using GC-MS and tested its effect on C. verum in conjunction with other major EO components reported in the literature, linalool, linalyl, and  $\beta$ -caryophyllene.

TCA and linalool mirror the effects of *C. verum* EO while linally acetate and  $\beta$ -caryophyllene, were mainly ineffective. Although we have identified some active components, we cannot discard that other -non-selected-compounds may exhibit anthelmintic activities. Indeed, eugenol, also detected in our EO sample, was previously reported to show anthelmintic properties<sup>38–40</sup>. *Cinnamomum verum* essential oil, at its IC50 value of 0.0175%

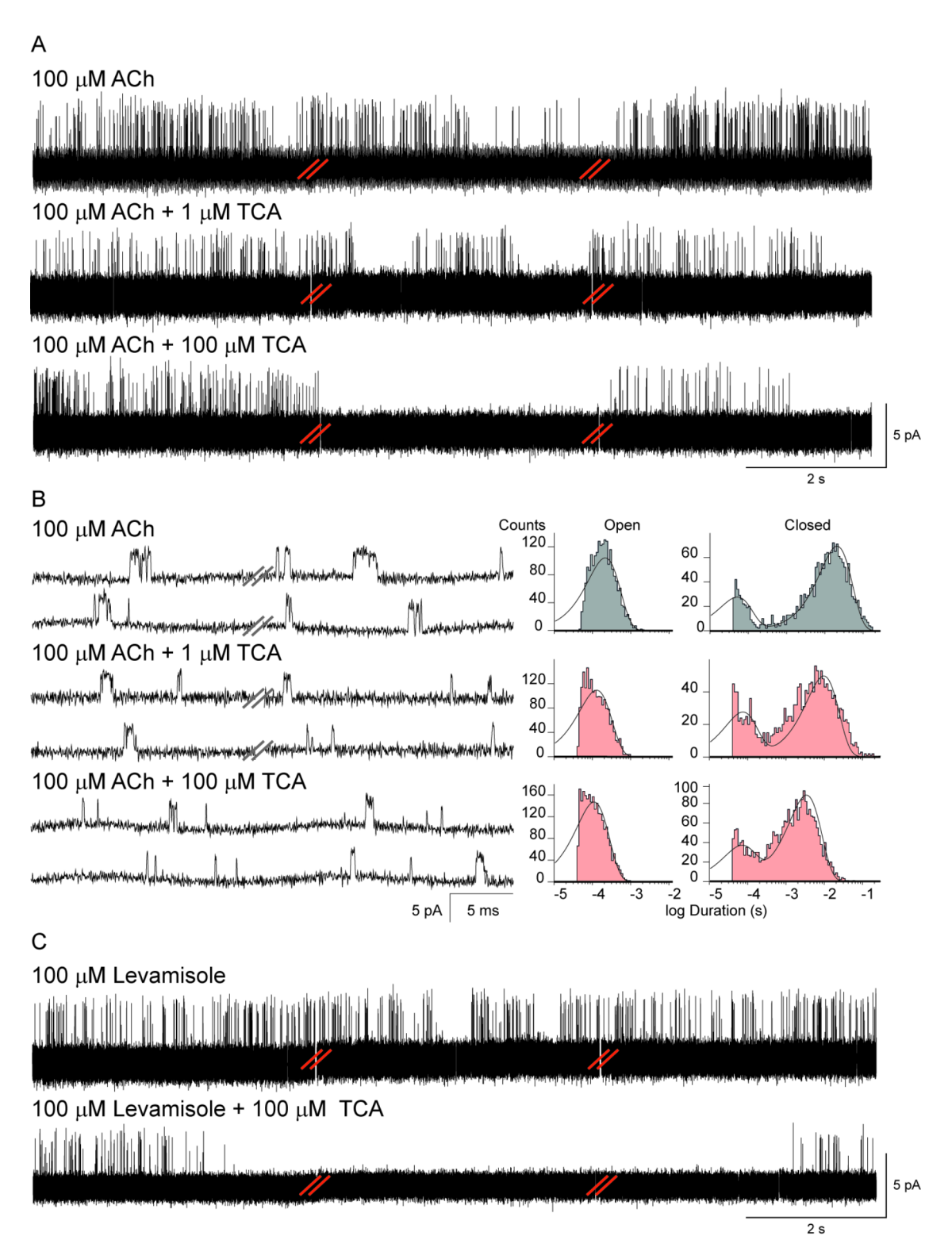


**Fig. 6.** Inhibitory effects of TCA on L-AChR channel activity. (A) L-AChR single-channels activated by 100  $\mu$ M ACh were recorded in the absence (top) and presence of 1  $\mu$ M and 100  $\mu$ M TCA (bottom). Three different traces of the same recording separated by red dashes are shown for each condition; the first trace corresponds to recording during the first minute and the other two traces, during the third minute. Channel openings are shown as upward deflections. Pipette potential: 100 mV. Filter: 9 kHz. (B) Representative traces and open and closed time histograms of channels recorded as explained in panel A. The long-closed periods were excluded from histograms as they were examined and calculated through inspection across all recordings (7–10 min). (C) L-AChR single-channels activated by 100  $\mu$ M levamisole were recorded in the absence (top) and presence of 100  $\mu$ M TCA (bottom). As described for ACh, three different traces separated by red dashes are shown for each condition. Pipette potential: 100 mV. Filter: 9 kHz.

Agonist	Treatment	O1 (ms) (area)	C1 (ms) (area)	C2 (ms) (area)	Burst (ms)	n
10 μM ACh	DMSO control	0.29 ± 0.01 (1)	0.037 ± 0.012 (0.24 ± 0.06)	52±35 (0.67±0.15)	$0.45 \pm 0.09$	8
	100 μM TCA	0.16±0.03 (1)	0.04±0.01 (0.34±0.09)	18±9 (0.58±0.31)	$0.20 \pm 0.08$	6
100 μM ACh	DMSO control	0.23 ± 0.04 (1)	0.057±0.012 (0.41±0.17)	32±25 (0.57±0.18)	0.37 ± 0.09	7
	1 μM TCA	0.12 ± 0.02 (1)	$0.03 \pm 0.009 \\ (0.52 \pm 0.09)$	14±10 (0.44±0.1)	$0.20 \pm 0.04$	7
	100 μM TCA	0.12±0.01 (1)	$0.057 \pm 0.01$ $(0.30 \pm 0.06)$	3.2 ± 0.44 (0.51 ± 0.19)	0.18 ± 0.018	5
100 μM LEV	DMSO control	0,27+0,04 (1+0)	0,05+0,016 (0,10+0,04)	35+7 (0,41+0,14)	0,33 + 0,05	7
	100 μM TCA	0,13+0,03 (1+0)	0,04+0,01 (0,34+0,09)	18+9 (0,58+0,31)	0,23 + 0,10	6

**Table 1**. L-AChR single-channel properties examined for ACh- and levamisole-activated channels in the absence and presence of TCA. Single channels were recorded from *C. elegans* L1 muscle cells at a pipette potential of 100 mV. L-AChR channels were recorded in the absence and presence of TCA. The mean durations of the open component (O1) and closed components (C1 and C2) and mean burst durations were obtained from the corresponding histograms. Data are shown as mean  $\pm$  SD and the number of recordings for each condition is indicated (n). LEV: Levamisole. Statistical comparison of burst activity showed *p* < 0.001 for 10 μM ACh (DMSO control) vs. 10 μM ACh + 100 μM TCA, 100 μM ACh (DMSO control) vs. 100 μM ACh + 100 μM TCA. Comparison of 100 μM LEV (DMSO control) and 100 μM LEV + 100 μM TCA showed *p* = 0.046.

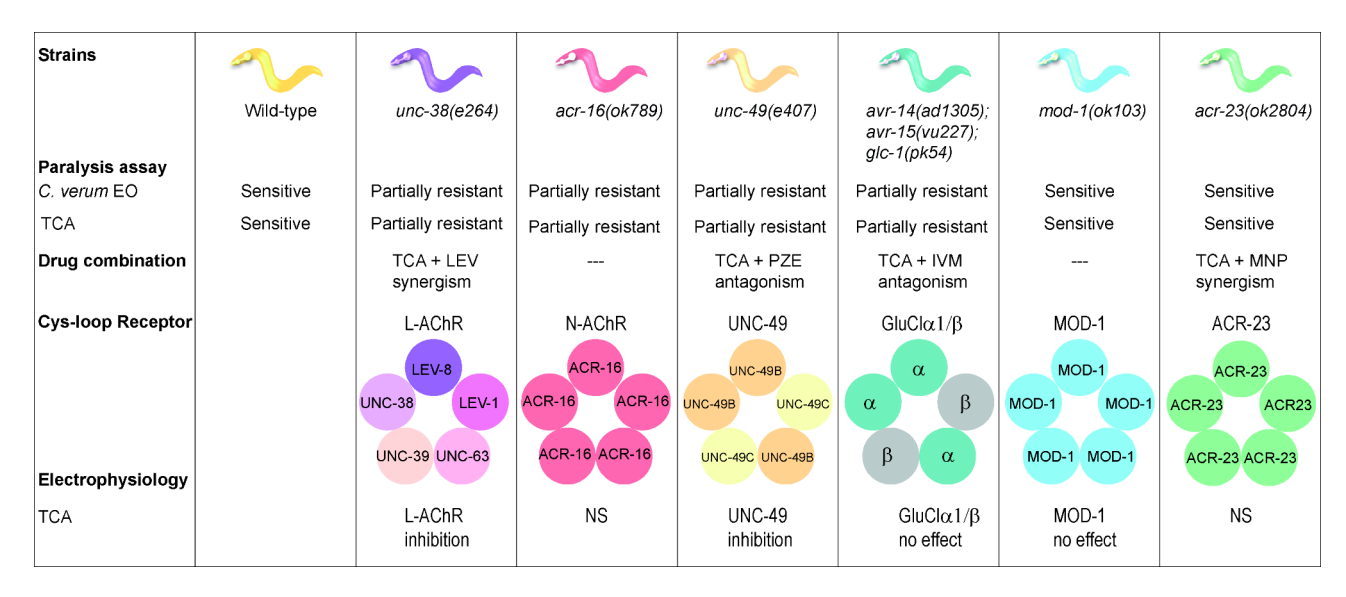


**Fig.** 7. Dissecting anthelmintic effects of *C. verum* EO and TCA on *C. elegans*. The figure represents the comprehensive analysis of *C. verum* EO and TCA conducted in our study from the organism to the molecular level, employing various mutant strains of crucial Cys-loop receptors. The figure shows: Results of the sensitivity to *C. verum* EO and TCA of wild-type and different mutants worms lacking functional key Cysloop receptors; the effects of TCA combinations with conventional anthelmintic drugs (LEV, levamisole; PZE, piperazine; IVM, ivermectin; MNP, monepantel); and the effects of TCA on receptor function evaluated by electrophysiological studies. NS: not studied.

(v/v), demonstrates potent anthelmintic activity against C. elegans, with concentrations of 0.332 mM TCA, 0.00321 mM linalool, and 0.00754 mM eugenol—lower than the IC50 values of the pure compounds. This indicates that the oil's activity cannot be attributed solely to individual components but likely results from additive or synergistic interactions among its constituents. These effects may involve complementary mechanisms of action, enhanced bioavailability, or stabilization of active compounds within the oil matrix. Minor components, such as linally acetate and  $\beta$ -caryophyllene, may also contribute to amplifying the oil's efficacy.

We show that *C. verum* EO, TCA and linalool induce paralysis of body wall muscles, leading to the suppression of head and tail movements, while maintaining the original length of worms. This denotes a distinct form of paralysis compared to levamisole, which induces sustained muscle contraction and spastic paralysis by activating L-AChR, leading to reduced worm length. This disparity may be attributed to the compounds functioning as

negative modulators rather than agonists of L-AChR. Furthermore, their multitarget nature suggests that the ultimate impact on body length may arise from the integrated effects across multiple receptors.

The identification of molecular targets stands as a crucial step in drug discovery. Therefore, drug screening of mutant strains provides a valuable approach to achieve this goal. In this study, we explore the effects of *C. verum* EO and TCA on selected mutant strains lacking Cys-loop receptors with importance in worm locomotion. The rationale is based on the fact that the lack of the molecular target generates resistance to the drug. The results suggest the involvement of GluCls, L-AChRs, N-AChRs, and UNC-49 receptors in the paralyzing effects of *C. verum* EO, TCA and linalool. However, neither mutant strain became totally resistant to the drug, indicating multiple contributions. In contrast, at the tested concentrations, TCA and linalool effectively reduce egg hatching in all mutant strains similarly to the wild-type strain. This activity could have potential for use against parasitic nematodes, including those resistant to commercial anthelmintics. Other potential targets, not explored in this study, may also contribute to the anthelmintic effects of TCA. In this regard, TCA and several other bioactive molecules have been shown to interact with receptors from diverse families, including transient receptor potential channels found in *C. elegans*<sup>41,42</sup>. Thus, it appears that bioactive molecules, which combine multiple activities within a single compound, may be implemented as a polypharmacological strategy with enhanced efficacy and reduced risk of drug-drug interactions<sup>43</sup>.

In addition to its multitargeting properties, we investigated the potential of TCA in polytherapy with conventional drugs, a strategy pivotal in modern clinical practice. Polytherapy combines drugs that act through distinct mechanisms within the same organism, enhancing efficacy and mitigating drug resistance development <sup>44</sup>. This approach is particularly crucial in combating the escalating challenge of resistance in antiparasitic therapy, affecting both animal and human health.

For combination therapies, we selected LEV, MNP, PZE, and IVM, which target Cys-loop receptors <sup>10</sup>, alongside TCA and examined them by paralysis assays on agar plates. Our results reveal strong synergistic effects with TCA/LEV and TCA/MNP combinations, which significantly enhanced worm paralysis compared to the sum of individual drugs. These findings are further supported by the CI values, where CI < 1 indicates synergism. Conversely, TCA exhibited antagonistic effects when combined with IVM or PZE (CI > 1 for both combinations), thus highlighting the critical need for careful drug selection and rigorous testing in model organisms. Our approach not only ensures the efficient development of effective combination therapies for anthelmintic treatments but also identifies antagonistic and ineffective combinations that reduce efficacy, thereby conserving valuable time and resources. Overall, our findings provide crucial insights for formulating successful anthelmintic treatments.

Building upon our findings from screening mutant strains that identified various Cys-loop receptors, our focus shifted towards unraveling the underlying mechanism of action. In our electrophysiological experiments, preincubation with TCA resulted in a reduction of macroscopic peak currents induced by endogenous agonists in L-AChR and UNC-49 receptors, indicating TCA's role as an inhibitor of these receptors at the neuromuscular junction. Notably, TCA exhibited a distinct mechanism of action from LEV and PZE, as evidenced by its inability to generate macroscopic currents in the absence of the corresponding agonists. A direct correlation between the TCA concentrations used in electrophysiological recordings with those used in paralysis assays is not expected due to several factors: (i) the whole-cell recordings from the cultured cells allow neither extended pharmacological studies nor exposure to high TCA concentrations over a relatively long time due to the instability of the patches; (ii) both the concentration and time of application of TCA in the electrophysiological experiments are smaller than those used to induce paralysis in the entire worm, for which absorption is required; and, (iii) TCA modulates different receptors simultaneously. These factors may explain the apparent controversy between the small effects on peak currents of GABA and L-AChR receptors and the paralysis induced by TCA. Nevertheless, the peak reductions align with the clear partial resistance of the mutant worms lacking these receptors.

TCA demonstrated no effect on the macroscopic currents of GluClα1/β elicited by glutamate when compared to the control. Six genes in *C. elegans* encode GluCl subunits: *avr-14* (GluClα3 subunit), *avr-15* (GluClα2), *glc-1* (GluClα1), *glc-2* (GluClβ), *glc-3* (GluClα4), and *glc-4*<sup>10</sup>. Our observation that the triple mutant strain *avr-14(ad1305);avr-15(vu227);glc-1(pk54)* exhibits partial resistance to TCA suggests the involvement of another GluCl subtype not explored in this study. Furthermore, TCA did not affect MOD-1 macroscopic currents, consistent with our paralysis assay findings, indicating that despite its multitarget feature, it does not modulate all Cys-loop receptors.

To explore the inhibitory effect of TCA on native L-AChRs, we performed single-channel recordings from L1 *C. elegans* muscle cells. Our study revealed a significant alteration in the channel activity pattern of L-AChRs, characterized by a higher occurrence of prolonged silent periods devoid of activity, which varied with TCA concentration. We developed a method to quantify this enhancement of channel inactivity by measuring the percentage of time with silent periods longer than 0.5 s relative to total recording time. The precise mechanism behind these prolonged closures, which could involve impaired opening, desensitization, or slow channel block, remains unclear.

Furthermore, our analysis of L-AChR single-channel properties in the presence of TCA shows reduced open channel and burst durations, along with shorter durations of the main closed state. The reduction in open duration is compatible with open channel block, but the changes in burst duration and main closed component duration suggest a block mechanism not consistent with fast open-channel block. Altogether, these observations suggest that TCA inhibits native L-AChRs through a complex mechanism, potentially involving allosteric inhibition and/or channel blockade.

The use of EO as anthelmintics shows promise against nematode parasites, with cinnamon bark extracts containing TCA proving effective<sup>6,7,18,22</sup>. However, challenges exist in practical applications for mammals, as orally administered EO, including carvacrol, thymol, and cinnamaldehyde, are quickly absorbed and metabolized

in the gastrointestinal tract<sup>22–24</sup>. This limits their availability, hindering their efficacy. Future research should focus on enhancing EO bioavailability and stability for better anthelmintic performance in mammals.

The safety and toxicity of *C. verum* and its primary component, TCA, have been extensively investigated. Safety assessments, including invertebrate and vertebrate animal trials and clinical studies, have determined the low toxicity of *C. verum*, supporting its potential as a safe therapeutic agent<sup>2,3,45–47</sup>. The collective evidence reinforces cinnamon's favorable safety profile, warranting consideration for health applications.

#### Conclusions

*C. verum* EO and its main bioactive components TCA and linalool exhibit potential anthelmintic activity. Our electrophysiological and behavioral studies examining TCA effects on *C. elegans* reveal that the marked anthelmintic effectiveness is mediated through modulation of several Cys-loop receptors. In particular, TCA acts as an inhibitor of two key receptors involved in nematode mobility; the L-AChR and the GABA-activated chloride channel (UNC-49). TCA combinations with other classical anthelmintics, particularly levamisole and monepantel, represent promising strategies for further antiparasitic drug research. The utilization of multi-target natural compounds in anthelmintic formulations holds potential as a novel therapeutic approach.

#### Materials and methods

Chemicals and essential oils: TCA, linalool, linalyl acetate,  $\beta$ -caryophyllene, levamisole, ivermectin, piperazine and DMSO (Sigma-Aldrich Co), monepantel (Zolvix, Elanco) and bark cinnamon EO, *C. verum* EO (Saiku, Argentina).

#### Caenorhabditis elegans strains

Nematode strains used were: N2: Bristol wild-type; PD4251: *ccIs4251;dpy-20(e1282)*; DA1316: *avr-14(ad1305);avr-15(vu227);glc-1(pk54)*; CB904: *unc-38(e264)*; RB918: *acr-16(ok789)*; CB407: *unc-49(e407)*; MT9668: *mod-1(ok103)*; RB2119: *acr-23(ok2804)*.

All nematode strains were obtained from the *Caenorhabditis* Genetics Center, Nematode strains were maintained as described in previous studies<sup>38</sup>.

#### Paralysis assays

Assays were performed with young adult hermaphrodites' worms from synchronized NGM plates. Paralysis was determined on fresh agar plates without bacteria and containing the tested drug or DMSO vehicle at room temperature as described in previous studies<sup>38</sup>. Paralysis was defined as the lack of movement in response to gentle prodding of the body as described previously<sup>35,48</sup>. All experiments were conducted in a blind manner.

For concentrations expressed in percentage (%) of *C. verum* EO, volume/volume (v/v) was considered. The stock solutions of TCA (370 mM), linalool (640 mM), linalyl acetate (500 mM), and  $\beta$ -caryophyllene (864 mM) were freshly prepared in DMSO on each experiment day. In all assays, DMSO concentrations were maintained below 1% (v/v), as this concentration is unlikely to interfere with the results<sup>49,50</sup>. However, higher DMSO concentrations (1–2%) were required for the conditions involving 7 mM linalyl acetate and 10 mM  $\beta$ -caryophyllene on agar plates. For these specific conditions, additional control groups with DMSO were included to ensure there were no significant differences compared to conditions without DMSO.

#### Motility assays

Motility assays were conducted utilizing the WMicroTracker (Phylumtech, Argentina) in liquid medium. Synchronized young adult hermaphrodite worms were transferred to flat bottomed 96-well microplates (about 50–60 worms per well in water) as described in previous studies $^{34}$ . Worms' basal movement (control of worms' movement) was measured for 30 min to normalize the movement activity for each well at the beginning of the assay (basal, 100% activity). Then, compounds were added to a final volume of 100  $\mu$ l per well and motility was analyzed in 5-min time bins during 60–120 min. For each well, the motility value at a given time (60–120 min) was related to the basal one. All compounds were tested with a minimum of twelve replicates per plate. For comparison among different concentrations, the assays were performed in parallel. Each condition was evaluated in at least five independent experiments with different synchronized worm batches and always in parallel with the respective control. The motility of the control group was consistently stable throughout the experiment, with no significant differences observed between the 0-hour and 2-hour time points.

## Body length measurement

For *C. elegans* body length measurements we used fresh-agar plates with or without *C. verum* EO or drugs. Assays were performed with its respective controls as described in previous studies<sup>38</sup>. Data are presented as the body length of *C. elegans* after drug exposure, normalized to the control group, where the control group is set as 1. At least three independent experiments were carried out for each condition. Levamisole was chosen for experimentation due to its significant ability to induce spastic paralysis, which can be easily quantified.

## C. elegans egg hatching assay

We determined the ability of drugs to inhibit egg hatching according to the method described previously<sup>27</sup>. The number of unhatched eggs and first-stage larvae or larva 1 (L1) was counted under a Stereoscopic Zoom Microscope.

#### C. elegans drug combinations assay

Synchronized young adult worms were transferred to agar plates containing individual commercial anthelmintics or TCA at varying concentrations, or three distinct combinations of TCA with each anthelmintic ( $n \ge 30$  worms per agar plate, 20 °C). Subsequently, the fraction of paralyzed worms was measured after 1 h of exposure. All experimental conditions were performed in parallel and compared to the control without drugs. Initially, several anthelmintic concentrations were tested in order to select concentrations that induce paralysis on agar plates in less than 50% of worms, following the assay protocol described in detail in reference<sup>51</sup> (the concentrations used for each experiment are indicated in the respective figures and/or their captions and/or supporting information).

Commercial anthelmintics: Levamisole, piperazine, monepantel, and ivermectin were chosen for experimentation due to their widespread commercial use against various parasitic nematodes in humans and animals. They were selected for their efficacy in targeting Cys-loop receptors, making them effective treatments for different nematode infections.

The Combination Index (CI) values were calculated using Chou-Talalay's CI theorem from CompuSyn software to provide a more accurate assessment of the combined effects<sup>52,53</sup>. Additive effects, synergism, and antagonism are indicated by values of CI = 1, < 1, and > 1, respectively.

## Gas Chromatography-Mass Spectroscopy (GC-MS)

The identification of the components of the *C. verum* EO was carried out at the Universidad Nacional del Sur, INQUISUR, using an Agilent 7890B Gas Chromatograph with a Mass Selective Detector (MSD) 5977 A and a HP5-MS UI (30 m x 0.25 mm x 0.25  $\mu$ m) column. The detector was operated under full scan chromatographic conditions (Scan Mode). The identification of the main components was achieved by comparing the molecular structure of detected chemical compounds with data from the NIST MS 2.0 Library of GC-MS. The BM: TCA, linalool, linalyl acetate and  $\beta$ -caryophyllene, were tested on paralysis assays on agar plates, automated thrashing assays, measurements of body lengths, and egg hatching assays.

#### Isolation and culture of C. elegans muscle cells

To dissect the molecular mechanisms, electrophysiological studies were conducted on *C. elegans* embryonic muscle cells. Larva 1 (L1) muscle cells were obtained from *C. elegans* eggs and grown following previously described methods<sup>54</sup> and electrophysiological experiments were performed 1–5 days after cell isolation<sup>10,35,38</sup>.

## Heterologous cell expression of GluCl and MOD-1 receptors

GluCl (GluCl $\alpha$ 1 and GluCl $\beta$  subunits) and MOD-1 (MOD-1) receptors were transiently expressed in BOSC 23 cells, which are modified HEK 293T cells. Cells were transfected by calcium phosphate precipitation with the subunit cDNAs (total 4  $\mu$ g/35 mm dish) as described in previous studies<sup>33,34</sup>. Cells were used for whole-cell recordings 2 to 3 days after transfection, time at which maximal functional expression levels are typically achieved.

#### Patch-clamp recordings

Patch-clamp recordings were performed on L1 cells to measure activity of native *C. elegans* Cys-loop receptors (L-AChR and UNC-49 receptors) or in HEK cells expressing *C. elegans* Cys-loop receptors (MOD-1 and GluCl). Recordings were carried out at 20 °C in the whole-cell configuration for macroscopic currents and in the cell-attached patch configuration for L-AChR single-channel currents as described in previous studies<sup>10,35,38</sup>.

Single channels were recorded at 100 mV pipette potential with 1-100 µM ACh in the pipette solution using the program Acquire as described before, the bath and pipette were also described previously<sup>35</sup>. Channels were analyzed using TAC program (Bruxton Corporation). Open- and closed-time histograms and burst duration histograms were plotted using a logarithmic abscissa and a square root ordinate and fitted to the sum of exponential functions by maximum likelihood using TACFit (Bruxton Corporation).

Macroscopic currents were recorded in the whole-cell configuration from *C. elegans* L1 muscle cells<sup>35</sup> or from BOSC-23 cells transfected with the corresponding receptor subunit cDNAs<sup>33,34</sup> with the Intracellular Solution (ICS) and Extracellular Solution (ECS) as described in the mentioned references. To elucidate the modulatory action of TCA, responses were evaluated following a preincubation protocol<sup>34</sup>. Briefly, after whole-cell formation, agonist-elicited currents (control currents) were first recorded by a pulse of ECS containing agonist at -50 mV holding potential. Second, TCA in ECS was applied during 1–2 min in the absence of agonist (preincubation protocol), third a second agonist pulse was applied (treated currents). The entire experiment concluded with the application of ECS for an additional 60–90 s period followed by another pulse of agonist to check for current recovery. The duration of the agonist pulse was specific for receptor appropriate activation. Treated currents and recovered currents after ECS wash, were normalized to currents elicited by agonist alone in the same cell (control current). The change in the amplitude of the treated current compared to the control one was normalized and averaged among different cells.

Stock solutions for TCA (370 mM) were freshly prepared in DMSO for each experiment day and the final DMSO concentration used in all assays was lower than 0.1%.

## **Statistics**

The experimental data are shown as mean values with standard deviation (mean  $\pm$  SD).

Statistical comparisons were done using the Student's t-test, one-way ANOVA followed by either Bonferroni's or Dunn's method for multiple comparison post-tests. A significance level of p < 0.05 was considered as statistically significant. All the tests were performed with SigmaPlot 12.0 (Systat Software, Inc.; http://www.systat.de/SPW 12\_2infoEN.html). Dose-response curves were fitted by a nonlinear regression function using SigmaPlot 12.0, from which the IC50 (half maximal inhibitory concentration) values were obtained and expressed as mean  $\pm$  SD.

## Data availability

Data is provided within the manuscript or supplementary information files.

Received: 8 August 2024; Accepted: 10 February 2025

Published online: 13 February 2025

#### References

- 1. Muhammad, D. & food, K. D. I. journal of & undefined. International Journal of Food Properties Cinnamon and its derivatives as potential ingredient in functional food-A review Dimas Rahadian Aji Muhammad & Koen Dewettinck. *Taylor & Francis* 20, 2237–2263 (2017). (2017).
- 2. Ranasinghe, P. et al. Medicinal properties of 'true' cinnamon (*Cinnamomum zeylanicum*): a systematic review. *BMC Complement. Altern. Med.* 13, 275 (2013).
- 3. Guo, J. et al. Advances in pharmacological effects and mechanism of action of cinnamaldehyde. Front. Pharmacol. 15, 1365949 (2024).
- 4. Sharifi-Rad, J. et al. Cinnamomum species: bridging Phytochemistry Knowledge, Pharmacological properties and Toxicological Safety for Health benefits. Front. Pharmacol. 12, (2021).
- 5. Błaszczyk, N., Rosiak, A. & Kałużna-Czaplińska, J. The potential role of Cinnamon in Human Health. Forests 12, 648 (2021).
- 6. Verdú, J. R. et al. Nontoxic effects of thymol, carvacrol, cinnamaldehyde, and garlic oil on dung beetles: a potential alternative to ecotoxic anthelmintics. *PLoS One.* **18**, e0295753 (2023).
- 7. Fabbri, J., Maggiore, M. A., Pensel, P. E., Denegri, G. M. & Elissondo, M. C. In vitro efficacy study of *Cinnamomum zeylanicum* essential oil and cinnamaldehyde against the larval stage of *Echinococcus Granulosus*. Exp. Parasitol. 214, 107904 (2020).
- 8. Zhang, L., qing, Zhang, Z., gang, Fu, Y. & Xu, Y. Research progress of trans-cinnamaldehyde pharmacological effects. *China J. Chin. Materia Med.* 40, 4568–4572 (2015).
- 9. Choudhary, S., Kashyap, S. S., Martin, R. J. & Robertson, A. P. advances in our understanding of nematode ion channels as potential anthelmintic targets. *Int. J. Parasitol. Drugs Drug Resist.* 18, 52–86 (2022).
- 10. Hernando, G., Turani, O., Rodriguez Araujo, N. & Bouzat, C. The diverse family of cys-loop receptors in *Caenorhabditis elegans*: insights from electrophysiological studies. *Biophys. Rev.* 15, 733–750 (2023).
- Sepúlveda-Crespo, D., Reguera, R. M., Rojo-Vázquez, F., Balaña-Fouce, R. & Martínez-Valladares, M. Drug discovery technologies: Caenorhabditis elegans as a model for anthelmintic therapeutics. Med. Res. Rev. 40, 1715–1753 (2020).
- Holden-Dye, L. & Walker, R. J. Anthelmintic drugs and nematicides: studies in Caenorhabditis elegans. WormBook 1–29 (2014). https://doi.org/10.1895/wormbook.1.143.2
- Walker, R. J. et al. Nematode pharmacology: neurotransmitters, receptors, and experimental approaches. Nematodes as Model. Organisms. https://doi.org/10.1079/9781789248814.0006 (2022).
- 14. Panda, S. K., Daemen, M., Sahoo, G. & Luyten, W. Essential oils as Novel Anthelmintic Drug candidates. *Molecules* 27, 8327 (2022).
- 15. Wells, C. W. Effects of essential oils on economically important characteristics of ruminant species: a comprehensive review. *Anim. Nutr.* 16, 1–10 (2024).
- 16. Kaplan, R. M. et al. Antiparasitic efficacy of a novel plant-based functional food using an *Ascaris suum* model in pigs. *Acta Trop.* **139**, 15–22 (2014).
- 17. Catani, L., Manachini, B., Grassi, E., Guidi, L. & Semprucci, F. Essential oils as nematicides in Plant Protection—A Review. *Plants* 12, 1418 (2023).
- Katiki, L. M. et al. Synergistic interaction of ten essential oils against Haemonchus contortus in vitro. Vet. Parasitol. 243, 47–51 (2017).
- 19. Macedo, I. T. F. et al. Anthelmintic effect of *Cymbopogon citratus* essential oil and its nanoemulsion on sheep gastrointestinal nematodes. *Revista Brasileira De Parasitol. Veterinária.* 28, 522–527 (2019).
- 20. Trailović, S. M., Marjanović, D. S., Nedeljković Trailović, J., Robertson, A. P. & Martin, R. J. Interaction of carvacrol with the *Ascaris suum* nicotinic acetylcholine receptors and gamma-aminobutyric acid receptors, potential mechanism of antinematodal action. *Parasitol. Res.* 114, 3059–3068 (2015).
- 21. Trailovic, S. M., Rajkovic, M., Marjanovic, D. S., Neveu, C. & Charvet, C. L. Action of Carvacrol on *Parascaris sp.* and Antagonistic Effect on Nicotinic Acetylcholine Receptors. *Pharmaceuticals* 14, 505 (2021).
- 22. Williams, A. R. et al. Anthelmintic activity of trans-cinnamaldehyde and A- and B-type proanthocyanidins derived from cinnamon (*Cinnamomum verum*). Sci. Rep. 5, 14791 (2015).
- Garcia-Bustos, J. F., Sleebs, B. E. & Gasser, R. B. An appraisal of natural products active against parasitic nematodes of animals. Parasit. Vectors. 12, 306 (2019).
- 24. Matté, E. H. C., Luciano, F. B. & Evangelista, A. G. Essential oils and essential oil compounds in animal production as antimicrobials and anthelminitics: an updated review. *Anim. Health Res. Rev.* 24, 1–11 (2023).
- 25. Geary, T. G., Sakanari, J. A. & Caffrey, C. R. Anthelmintic Drug Discovery: into the future. J. Parasitol. 101, 125-133 (2015).
- 26. Lanusse, C. et al. Strategies to optimize the efficacy of Anthelmintic Drugs in ruminants. Trends Parasitol. 34, 664-682 (2018).
- Hernando, G. & Bouzat, C. Evaluating anthelmintic activity through Caenorhabditis elegans egg hatching assay. MethodsX 12, 102743 (2024).
- 28. Rana, P. & Sheu, S. C. Discrimination of four *Cinnamomum* species by proximate, antioxidant, and chemical profiling: towards quality assessment and authenticity. *J. Food Sci. Technol.* **60**, 2639–2648 (2023).
- 29. Lu, L. et al. Insecticidal activity and mechanism of cinnamaldehyde in C. elegans. Fitoterapia 146, 104687 (2020).
- 30. Ropiak, H. M. et al. Structure-activity relationship of condensed tannins and synergism with trans-cinnamaldehyde against *Caenorhabditis elegans. J. Agric. Food Chem.* **64**, 8795–8805 (2016).
- 31. Khadke, S. K., Lee, J. H., Kim, Y. G., Raj, V. & Lee, J. Appraisal of Cinnamaldehyde Analogs as Dual-Acting Antibiofilm and Anthelmintic agents. Front. Microbiol. 13, 818165 (2022).
- 32. Peden, A. S. et al. Betaine acts on a ligand-gated ion channel in the nervous system of the nematode *C. elegans. Nat. Neurosci.* 16, 1794–1801 (2013).
- 33. Castro, M. J., Turani, O., Faraoni, M. B., Gerbino, D. & Bouzat, C. A new antagonist of *Caenorhabditis elegans* Glutamate-activated Chloride channels with anthelmintic activity. *Front. Neurosci.* 14, 879 (2020).
- 34. Rodriguez Araujo, N., Hernando, G., Corradi, J. & Bouzat, C. The nematode serotonin-gated chloride channel MOD-1: a novel target for anthelmintic therapy. *J. Biol. Chem.* 298, 102356 (2022).
- 35. Hernando, G., Bergé, I., Rayes, D. & Bouzat, C. Contribution of subunits to *Caenorhabditis elegans* levamisole-sensitive nicotinic receptor function. *Mol. Pharmacol.* 82, 550–560 (2012).
- 36. Rayes, D., Flamini, M., Hernando, G. & Bouzat, C. Activation of single nicotinic receptor channels from *Caenorhabditis elegans* muscle. *Mol. Pharmacol.* 71, 1407–1415 (2007).
- 37. Lozon, Y. et al. Inhibition of human α7 nicotinic acetylcholine receptors by cyclic monoterpene carveol. *Eur. J. Pharmacol.* **776**, 44–51 (2016).
- 38. Hernando, G., Turani, O. & Bouzat, C. Caenorhabditis elegans mcysle Cys-loop receptors as novel targets of terpenoids with potential anthelmintic activity. PLoS Negl. Trop. Dis. 13, e0007895 (2019).

- 39. ElGhannam, M., Dar, Y., ElMehlawy, M. H., Mokhtar, F. A. & Bakr, L. Eugenol; Effective Anthelmintic Compound against Foodborne Parasite *Trichinella spiralis* Muscle Larvae and Adult. *Pathogens* 12, 127 (2023).
- Boyko, O. & Brygadyrenko, V. Survival of Nematode Larvae after treatment with Eugenol, Isoeugenol, Thymol, and Carvacrol. Front. Bioscience-Elite. 15, 25 (2023).
- 41. Xu, H., Delling, M., Jun, J. C. & Clapham, D. E. Oregano, thyme and clove-derived flavors and skin sensitizers activate specific TRP channels. *Nat. Neurosci.* 9, 628–635 (2006).
- 42. Yeon, J. et al. A sensory-motor neuron type mediates proprioceptive coordination of steering in *C. elegans* via two TRPC channels. *PLoS Biol.* **16**, e2004929 (2018).
- 43. Ryszkiewicz, P., Malinowska, B. & Schlicker, E. Polypharmacology: promises and new drugs in 2022. *Pharmacol. Rep.* **75**, 755–770 (2023).
- 44. Geary, T. G. et al. World Association for the Advancement of Veterinary Parasitology (W.A.A.V.P.) Guideline: Anthelmintic combination products targeting nematode infections of ruminants and horses. Vet. Parasitol. 190, 306–316 (2012).
- 45. Almatroodi, S. A. et al. Cinnamon and its active compounds: a potential candidate in disease and tumour management through modulating various genes activity. *Gene Rep.* 21, 100966 (2020).
- 46. da Alves, D. et al. N. Toxicological Parameters of a Formulation Containing Cinnamaldehyde for Use in Treatment of Oral Fungal Infections: An In Vivo Study. *Biomed Res Int* 1–13 (2021). (2021).
- 47. Ranasinghe, P. et al. *Cinnamomum zeylanicum* (Ceylon cinnamon) as a potential pharmaceutical agent for type-2 diabetes mellitus: study protocol for a randomized controlled trial. *Trials* 18, 446 (2017).
- 48. Almedom, R. B. et al. An ER-resident membrane protein complex regulates nicotinic acetylcholine receptor subunit composition at the synapse. *EMBO J.* **28**, 2636–2649 (2009).
- Boyd, W. A., Smith, M. V., Kissling, G. E. & Freedman, J. H. Medium- and high-throughput screening of neurotoxicants using C. elegans. Neurotoxicol Teratol. 32, 68–73 (2010).
- Lee, S. Y. & Kang, K. Measuring the effect of chemicals on the growth and reproduction of Caenorhabditis elegans. J. Visualized Experiments 128, e56437 (2017).
- 51. Hernando, G. & Bouzat, C. Drug combination assays using Caenorhabditis elegans as a model system. J. Pharmacol. Toxicol. Methods. 131 https://doi.org/10.1016/j.vascn.2025.107583 (2025).
- 52. Chou, T. C. & Martin, N. CompuSyn for Drug Combinations: PC Software and User's Guide: A Computer Program for Quantitation of Synergism and Antagonism in Drug Combinations, and the Determination of IC50 and ED50 and LD50 Values. *ComboSyn Inc, Paramus* Preprint at www.combosyn.com (2005).
- 53. Chou, T. C. & Theoretical Basis Experimental design, and Computerized Simulation of synergism and antagonism in Drug Combination studies. *Pharmacol. Rev.* **58**, 621–681 (2006).
- 54. Christensen, M. et al. A Primary Culture System for Functional Analysis of *C. elegans* neurons and muscle cells. *Neuron* 33, 503–514 (2002).

## **Acknowledgements**

We express our gratitude to Dr. Werdin Gonzalez (INBIOSUR, Arg.) for generously providing the linalool, linalyl acetate and  $\beta$ -caryophyllene and to Dr. Carlos Lanusse (CIVETAN, Arg.) for kindly providing the monepantel. We were grateful to Dr. Paas (Bar-Ilan University, Israel) for generously providing the GluCl subunits and Dr. Horvitz (Massachusetts Institute of Technology, USA) for providing the cDNA encoding the MOD-1. We thank Wormbase. Strains were provided by the Caenorhabditis Genetics Center (CGC), which is funded by NIH Office of Research Infrastructure Programs (P40 OD010440).

#### **Author contributions**

G.H: conceptualization, supervision formal analysis, investigation, methodology, visualization, writing – original draft, review and editing, funding acquisition. O.T: methodology, investigation, visualization. N.R.A: methodology, investigation, visualization. C.B: conceptualization, supervision formal analysis, writing, review and editing, funding acquisition. All authors reviewed the manuscript.

#### Funding

This work was supported by Argentine grants from Agencia Nacional de Promoción de la Investigación, el Desarrollo Tecnológico y la Innovación (PICT 2019–01751 to GH and PICT 2020–00936 to CB), Consejo Nacional de Investigaciones Científicas y Técnicas (CONICET, PIP11220200102356) and Universidad Nacional del Sur (PGI 24/B340 to GH and PGI 24/B298 to CB).

## **Declarations**

## Competing interests

The authors declare no competing interests.

## Additional information

**Supplementary Information** The online version contains supplementary material available at https://doi.org/1 0.1038/s41598-025-89883-4.

Correspondence and requests for materials should be addressed to G.H.

Reprints and permissions information is available at www.nature.com/reprints.

**Publisher's note** Springer Nature remains neutral with regard to jurisdictional claims in published maps and institutional affiliations.

Open Access This article is licensed under a Creative Commons Attribution-NonCommercial-NoDerivatives 4.0 International License, which permits any non-commercial use, sharing, distribution and reproduction in any medium or format, as long as you give appropriate credit to the original author(s) and the source, provide a link to the Creative Commons licence, and indicate if you modified the licensed material. You do not have permission under this licence to share adapted material derived from this article or parts of it. The images or other third party material in this article are included in the article's Creative Commons licence, unless indicated otherwise in a credit line to the material. If material is not included in the article's Creative Commons licence and your intended use is not permitted by statutory regulation or exceeds the permitted use, you will need to obtain permission directly from the copyright holder. To view a copy of this licence, visit <a href="http://creativecommons.org/licenses/by-nc-nd/4.0/">http://creativecommons.org/licenses/by-nc-nd/4.0/</a>.

© The Author(s) 2025